# Enhanced Sizing Methodology for the Renewable Energy Sources and the Battery Storage System in a Nearly Zero Energy Building

Evangelos Tsioumas, *Student Member, IEEE*, Nikolaos Jabbour, Markos Koseoglou, *Student Member, IEEE*, Dimitrios Papagiannis, *Student Member, IEEE*, and Christos Mademlis, *Senior Member, IEEE*

***Abstract*—The aim of this article is to present a novel methodology to determine the correct size of the renewable energy sources (RES) and the battery storage system (BSS) that are needed to effectively convert a conventional residential building into a nearly zero-energy building (nZEB). This is attained by properly considering the long-term history of the weather at the location of the building, the energy consumption of the appliances and the performance of the energy management system (EMS). The above are embedded in a cost function that balances the impact factors which highly affect the size and have considerable effect on the reliability and lifespan of the RES and BSS in a nZEB, i.e., the depreciation of the initial investment, the self-consumption rate, the feed-in rate, the simultaneity in generating and consuming power, and the impacts of the depth-of-discharge and the discharge power on the BSS's state-of-health. Therefore, the correct sizing of RES and BSS is provided by considering both the effectiveness and the economic point of views. Specifically, the optimal solution is attained by minimizing the above cost function through the genetic algorithm technique. The effectiveness, functionality and practicality of the proposed methodology have been validated on a pilot nZEB.**

***Index Terms*—Efficiency increase, energy sizing, energy storage, nearly-zero energy building, power sizing, renewable energy generation, resource planning, solar system, wind system.**

## I. Introduction

As THE nature of the urban buildings is changing from static and passive structures to active and dynamic environments for living and working, there is a rapidly increasing energy demand reaching to an average of 40% of total end-use energy and with values of up to 90% in densely populated regions [1]. At the same time, the smart building concept has transformed from conceptual to operational, while the evolution in the communication infrastructures and the processing tools has increased the efficiency in the exploitation of the generated electric power.

Since the energy consumption in buildings is expected to have an increasing trend in the next decades, several measures have been taken by the authorities to restrain it, such as the directives 2002/2018 [2] and 844/2018 of the European Union [3]. The above measures aim to the development of an efficient, secure and decarbonized energy system. Thus, the encouragement for the adoption of the nearly zero-energy building (nZEB) for the buildings will have a key role in the success of the efforts toward a sustainable future.

As a definition for the nZEB is that, it is a building with high energy performance and the nearly zero or very low amount of the required energy is provided by RES generated on-site or nearby [4]. The commonly used RES for nZEBs are photovoltaics (PVs) and small wind turbines (WTs) [5]. The reduction in the energy consumption can be attained through an EMS by considering the weather conditions and using high energy efficiency appliances [6]. Heating, ventilation, and air conditioning systems of improved performance, in conjunction with heat-pumps (HPs), can be used to further improve the nZEB's energy efficiency and reduce or possibly eliminate the fossil-fuel usage and the building's carbon footprint [7]. Moreover, the utilization of a BSS may be considered as inseparable part in the efforts of effectively deploy and take full advantage of the nZEB benefits [8].

The EMS has a crucial role on the performance of an nZEB, since it is responsible for the appropriate scheduling of the manageable appliances according to the generated energy by the RES and the proper exploitation of the BSS capabilities, as well as, the effective protection of the batteries (BTs) lifespan [9]. The fulfillment of the above objectives can lead to the effective peak shaving of the energy consumption, the enhancement of the stability and the seamless operation of the building's microgrid, as well as, it can contribute to the cost-effectiveness of the nZEB's operation [10].

From the above it is concluded that the future of the nZEB is closely tied with the proper utilization of the RES and BSS [11]. However, since the purchase and installation of the RES and BSS in order to convert a conventional building to nZEB entail an initial investment cost, the correct sizing of the above equipment with respect to the expected operational energy cost reduction of the building is an important issue [12]. Specifically, the correct

Manuscript received September 10, 2020; revised December 23, 2020; accepted February 3, 2021. Date of publication February 10, 2021; date of current version June 1, 2021. This work was supported by the European Union and Greek national funds through the Operational Program Competitiveness, Entrepreneurship, and Innovation, under the call RESEARCH–CREATE–INNOVATE under Project T1EDK-00399. Recommended for publication by Associate Editor W. Cao. *(Corresponding author: Nikolaos Jabbour.)*

The authors are with the Department of Electrical and Computer Engineering, Aristotle University of Thessaloniki, Thessaloniki 54124, Greece (e-mail: etsioumas@ece.auth.gr; njabbour@auth.gr; markkose@ece.auth.gr; dipapagi@auth.gr; mademlis@auth.gr).

Color versions of one or more of the figures in this article are available online at https://doi.org/10.1109/TPEL.2021.3058395.

Digital Object Identifier 10.1109/TPEL.2021.3058395

selection of the nominal power and energy, the proper technical characteristics, the appropriate mixture of PVs and WTs, and the configuration of BSS should be carefully determined, so as the decision on the energy upgrade of a building to nZEB can provide the expected operational and economic benefits [13].

On the contrary, a potential incorrect selection of the RES and BSS as separate units or as a combined system may not only result to the nZEB performance deterioration and thus, the investment failure, but it may escalate the problem of wasting energy resources. This may also have broader consequences in the projection of the nZEB's concept resulting in the overall discrediting of the effort [14]. Moreover, since the production of RES and BSS devices consumes valuable environmental resources, the failure of the nZEB to provide the expected benefits aggravates the environmental problems instead of solving them [15]. Therefore, the correct sizing of the RES and BSS, and the proper design of the nZEB's microgrid are key elements toward a cost-efficient equilibrium between the decarbonization in the energy supply and the reduction in the energy consumption.

Due to the high importance of the correct sizing of the nZEB's equipment, considerable research interest has been attracted. Moreover, specific consideration has been given to installations in remote areas or weak network infrastructures. A multiobjective method for a stand-alone system in order to determine the correct size of PVs, WTs and BSS has been proposed in [16], aiming to the complementary usage of PVs and WTs for the cost minimization and the high supply reliability. The total cost per year to optimize the selection of the system components by using the particle-swarm-optimization technique, has been examined in [17]. The genetic algorithm (GA) technique has been employed in [18] to properly select the size of the RES, while a diesel generator was used as a complementary energy source. An attempt for the optimal design and the techno-economic analysis, aiming to increase the RES penetration has been presented in [19]. The proposed methodology can provide considerable fossil-fuel power reduction; however, it is focused on the autonomous small isolated microgrids and not on nZEBs. Also, security-constrained issues with respect to the proper technology mix, size, placement and associated dispatch have been studied in [20]; however, they are referred to isolated multi-energy microgrids and not to nZEBs. The total life-cycle cost and the potential carbon emissions have been considered as criteria for the calculation of the correct sizing of the nZEB's equipment in [21]. However, it has not been included in the study the case that the electric energy generated by RES cannot be self-consumed, due to low energy demand by the building, and cannot be absorbed by the grid, due to its energy saturation. A methodology for the proper sizing of RES and BSS for a stand-alone nZEB has been proposed in [22], by considering as criteria the initial investment and the potential maintenance costs, while the information for the weather conditions are obtained by historical data.

In recent years, the emergence of the smart-grid, the high penetration by distributed RES, and the several economic opportunities that the electricity market may provide have featured the significant impacts of the equipment configuration and the EMS on the nZEB performance. The impact of the size of the PV, WT, and BSS on an nZEB microgrid performance have been examined in [23], by considering the average of solar and wind condition data at the installation site, and the annual operating cost of the building. A mixed integer linear programming approach that determines the optimal portfolio of RES, size, placement and associate dispatch, based on the DER-CAM model, has been proposed in [24]. However, it was focused on multi-energy microgrids and not on nZEBs. A calculation model for the proper size of the BSS has been proposed in [25], while the RES have been arbitrarily selected. The proper design of a PV-biomass gasifier-diesel and grid base hybrid system for different load profiles, by utilizing the HOMER software, has been presented in [26]. The proposed methodology is focused on grid-scale microgrids and, although it admits the importance of the load shifting for the reduction of the cost of energy generation cost, it ignores it in the analysis. The impacts of several operating variables on the proper determinization of the sizing of a hybrid power system with PVs, WTs, and BTs have been examined in [27]; however, the effect of the EMS has not been considered. An extend approach of the DER-CAM model that incorporates electrical and thermal storage options has been presented in [28]; however, both the EMS performance and the BSS health degradation have not been considered. Sizing guidelines for the BSS, for an nZEB with preinstalled the PVs, have been presented in [29]. Finally, the impacts of several pricing mechanisms with respect to the proper sizing of PVs and BSS for an nZEB have been examined in [30].

Summarizing the above, although a considerable number of interesting research efforts have been conducted toward the correct sizing of the nZEB's equipment, several configuration variables and operating parameters that considerably affect the optimal solution have been disregarded. Specifically, most of the published research works consider the RES as a single entity and they do not determine the optimal sizing of separately the PVs and WTs. Some of them are based on the average monthly and yearly energy data, and they ignore several operating cases that may affect the optimal sizing of the nZEB's equipment, such as the rate occurrence of the peak load demand. Moreover, potential cases that the generated energy by RES could not be consumed within the building's microgrid or absorbed by the grid or stored in BTs have not been considered in the calculations.

Although several of the published methods in the technical literature consider the energy capacity of the BSS, they disregard the nominal power in the calculations resulting in considerable inaccuracies, since the BSS power has a key role in the effective nZEB microgrid performance and also, considerably affect the cost of the system. Moreover, they ignore several important parameters of the BSS performance, such as the DoD and SoH, that considerably affect not only the effectiveness of the nZEB microgrid, but also the lifespan of the BSS. Finally, the published methodologies do not consider the EMS's performance on the regulation of the energy loads with respect to the grid's tariff policies. The above may result to either overestimation of the nZEB's equipment with respect to the real needs and consequently higher investment cost and lower exploitation, or underestimation that may lead to unsatisfactory performance of the nZEB.

Therefore, a comprehensive method is needed to address the problem of the correct sizing of the nZEB's equipment, from both effectiveness and economic aspects of RES and BSS, and also, considering the performance of the EMS and the protection of the BTs lifespan. The models of the RES, BSS, thermal, and EMS from both economic and technical point of views that are used in this article have been selected by considering a proper balance between the computational complexity and the desired accuracy. However, more accurate models can be utilized, by taking into account the above criteria. The nominal power of the PV and WT, and the nominal power and energy capacity of the BSS, as well as their technical characteristics are determined by considering the most important parameters that may affect the nZEB performance, i.e., the geographical and climate characteristics of the location, the loads energy demand, the depreciation of the initial investment, the self-consumption rate, the tariff policy in buying and selling electric energy by the grid, the rate in either generating or consuming electric energy, and the impacts of the DoD and the discharge power on the SoH variable of the BSS. Moreover, the performance of the EMS is considered through an emulation model in the form of virtual load shifting of the controllable appliances (CAs) for taking into account the energy management when peak load demand occurs and the optimal utilization of the generated energy by RES by properly selecting to be self-consumed by the nZEB, provided to the grid or temporarily stored to the BTs.

The proposed method is implemented by utilizing the GA technique and the enhanced solution is resulted through the minimization of a properly defined cost function that balances the impact factors of the optimization variables. The GA has been adopted in this work, since it can effectively solve the complicated objective functions of the examined problem. However, any other heuristic algorithms could be utilized but with the proper modifications, such as the swarm intelligence or the adaptive neural networks. A pilot nZEB at an urban area at Macedonia, Greece has been utilized to validate the effectiveness, functionality and practicality of the proposed methodology.

## II. Overview of the Proposed Methodology for the Correct Sizing of the RES and BSS

As can be seen in the schematic representation of Fig. 1, a typical nZEB' microgrid comprises: the RES with the power converters (usually PVs and WTs), a BSS, the EMS with the human machine interface, appropriate temperature sensors, energy meters, controllable switches and the appliances. The BSS is usually of Lead-acid or Li-ion BTs [31]. Although the Li-ion BTs are more expensive, they exhibit considerably improved technical characteristics with respect to the power, energy density and lifecycle that make them more suitable candidates for nZEB applications.

The EMS regulates the operation of the RES, BSS and appliances, in order to properly manage the electric energy within the nZEB's microgrid according to several predefined optimization objectives. Thus, several input signals (i.e., indoor and outdoor temperature, and energy consumption) and information data (i.e., weather forecast, residents' preferences, and real time buying and selling energy prices) are provided to the EMS.

Since the equipment that is needed to convert a conventional building to an integrated nZEB is costly, in some cases the full installation is not applied. This may confine the energy saving and reduce the energy autonomy level of the building. In this article, the sizing of the RES and BSS for the case of full nZEB's equipment installation is considered. However, since the proposed methodology is based on the minimization of a cost function structured by the impacts of specific optimization variables, there is high flexibility in adapting it according to the exact configuration of the desired nZEB and correctly selecting the values of the weighted factors.

The appliances can be classified in programmable, controllable and unschedulable. The programmable appliances (PAs) are electric loads that their operating time can be planned by the EMS (such as the electric cooker, the washing machine, dishwasher, ironing, vacuum cleaner, etc.). The CAs are electric loads that their operation is regulated by one or more variables (such as the heat pump, the air-conditioner, etc., where control variable is the temperature). The unschedulable appliances (UAs) are electric loads that cannot be programmed and they are switched ON/OFF either manually by the residents (such as the personal computers, TV, security lighting, etc.) or automatically (such as the lights regulated by a movement control system) and also, they are appliances that the residents do not have any control action (such as the refrigerator, water cooler, the controller board of the ICS, etc.).

The solution which is provided by the proposed algorithm, is the nominal power of the PVs and WTs, the nominal power and energy capacity of the BSS as well as the technical characteristics of the above equipment. The solution of the algorithm is determined by considering several operational parameters and economic variables, the history of the energy consumption, the geographical and climate characteristics of the location, and the impact of the EMS performance with respect to the desired energy autonomy level of the nZEB.

The overview block diagram of the proposed sizing methodology of the nZEB's equipment is illustrated in Fig. 2. It can be separated in four parts:

1) acquisition of the input data;
2) development of the model of the nZEB's equipment;
3) formulation of the cost function with respect to the optimization variables and definition of the weighted factors according to the desired energy autonomy level;
4) optimization process based on the GA technique, and finally, export of the results.

## III. Modeling of the nZEB Microgrid

In the proposed sizing algorithm of an nZEB's equipment, the PVs and WTs are used as RES, the BSS consists of Li-ion BTs and a heat pump is used for heating/cooling. The mathematical models of the above devices, as well as, the impacts of the EMS's performance and the cost and energy pricing models, are given later.

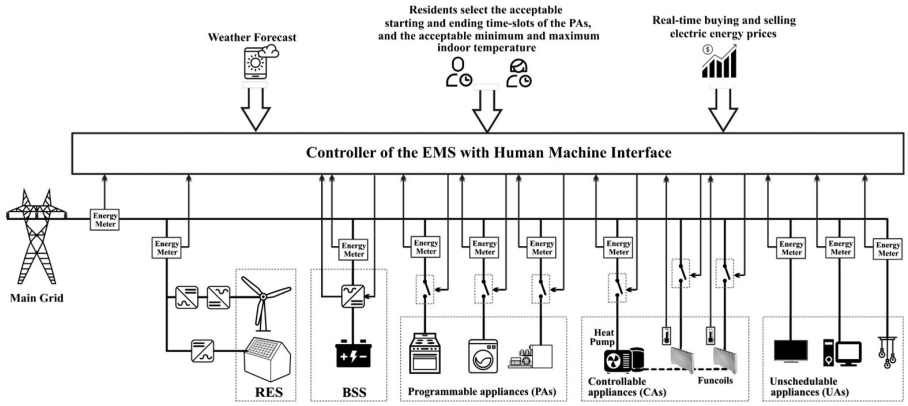


Fig. 1. Schematic representation of the examined nZEB.

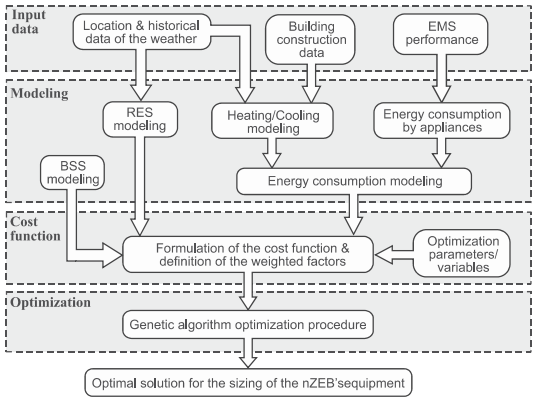


Fig. 2. Block diagram of the proposed methodology for the calculation of the enhanced sizing methodology of the nZEB's equipment.

### A. Power Model of a WT System

The mechanical power provided by a WT is given by [32]

$$P_{\mathrm{WT}} = \begin{cases} 0.5\rho A_{\mathrm{WT}} C_{P_{\max}} u_h^3 & u_{ci} < u_h < u_N \\ P_N & u_N \le u_h \le u_{co} \\ 0 & u_h > u_{co} \end{cases} \quad (1)$$

where $\rho$ is the air density, $A_{\mathrm{WT}}$ is the blades sweep area, $C_{P_{\max}}$ is the maximum aerodynamic coefficient (it is considered that the WT operates at the maximum power point), $u_h$ is the wind speed at the hub height, and $u_{ci}$, $u_{N,}$ and $u_{co}$ are the cut-in, nominal and cut-out wind speeds, respectively. The $P_N$ is the nominal electric power that is obtained from the nominal up to the cut-out wind speeds $(u_N \le u_h \le u_{co})$, while for higher wind speeds $(u_h > u_{co})$, the WT stops to provide electric energy.

The estimated electric power generated by a WT is based on the wind speed forecast $u_d$ that is given for a specific altitude above the see $h_d$. Thus, the Hellmann's exponential approach is utilized to determine the wind speed at the hub height [33], as given by

$$u_h = u_d (h_h / h_d)^{\gamma} \quad (2)$$

where $h_h$ is the hub height and $\gamma$ is the friction coefficient that depends on the roughness of the terrain [34], e.g., $\gamma = 0.3$ for small town with trees and shrubs, $\gamma = 0.4$ for large city with tall buildings, etc.

Considering the efficiency coefficients of the mechanical and the electrical parts of a WT ($\eta_{\mathrm{WT}m}$ and $\eta_{\mathrm{WT}e}$, respectively), the electric power that is provided to the nZEB microgrid is

$$P_{\mathrm{WT}e} = P_{\mathrm{WT}}\, \eta_{\mathrm{WT}m}\, \eta_{\mathrm{WT}e}. \quad (3)$$

### B. Power Model of a PV System

The PV output power, taking into account the temperature variations and the irradiance influence, can be calculated by the following equation [35]:

$$P_{\mathrm{PV}} = N_{\mathrm{PV}} \left\{ P_{\mathrm{PVmax}} \frac{R\mathrm{irr}}{1000} \left[ 1 - a_T (T_{\mathrm{PV_{cell}}}^{\mathrm{avg}} - 25) \right] \right\} \quad (4)$$

where $N_{\mathrm{pv}}$ is the number of the PV modules, $P_{\mathrm{PVmax}}$ is the peak output power of a PV module, $R_{\mathrm{irr}}$ is the irradiance level, $a_T$ is the temperature effect coefficient and $T_{\mathrm{PV_{cell}}}^{\mathrm{avg}}$ is the average temperature of the modules, which can calculated utilizing the nominal operating cell temperature model by the following expression [36]

$$T_{\mathrm{PV_{cell}}}^{\mathrm{avg}} = T_{\mathrm{amb}} + \left( \frac{T_{\mathrm{nom}} - 20}{800} \right) R_{\mathrm{irr}} \quad (5)$$

where $T_{\mathrm{amb}}$ is the ambient temperature and $T_{\mathrm{nom}}$ is the nominal operating cell temperature measured under standard environmental conditions (the irradiance level is 800 W/m$^2$, the ambient temperature is 20 °C, and the wind speed is 1 m/s).

Considering the efficiency coefficient of the PV power converter $\eta_{PV}$, the electric power that is provided to the nZEB microgrid is

$$P_{\mathrm{PV}e} = P_{\mathrm{PV}}\, \eta_{\mathrm{PV}}. \quad (6)$$

Note that the estimation of the generated power by RES for the proper sizing through the proposed method is based on historical data of the wind speed and irradiance. The use of predictive and artificial neural network methods can provide additional information and improve the accuracy of the WT and PV modeling [37], [38]; however, the computational complexity may be increased. Nevertheless, in case that higher accuracy

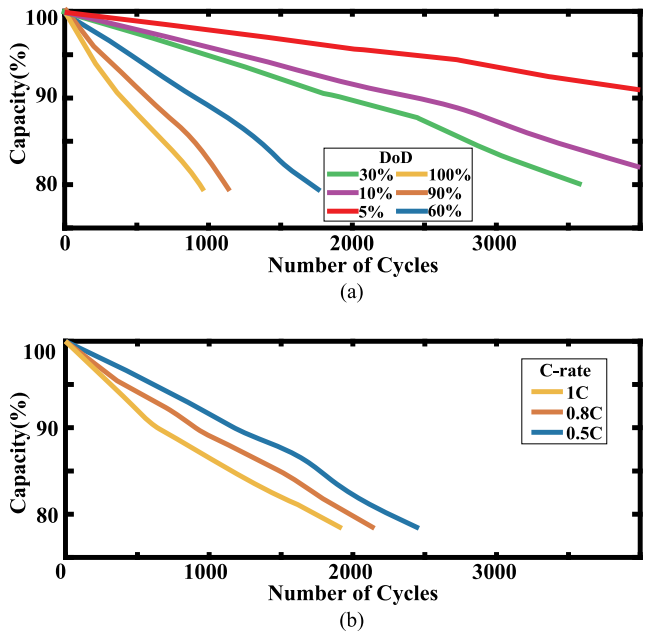


Fig. 3. Typical characteristic curves of the variation of the energy capacity versus the total equivalent life cycles of a Li-ion BT, for constant operating temperature 35 °C, for (a) several DoD values and constant 0.5C and (b) several C-rate values and constant 50% DoD.

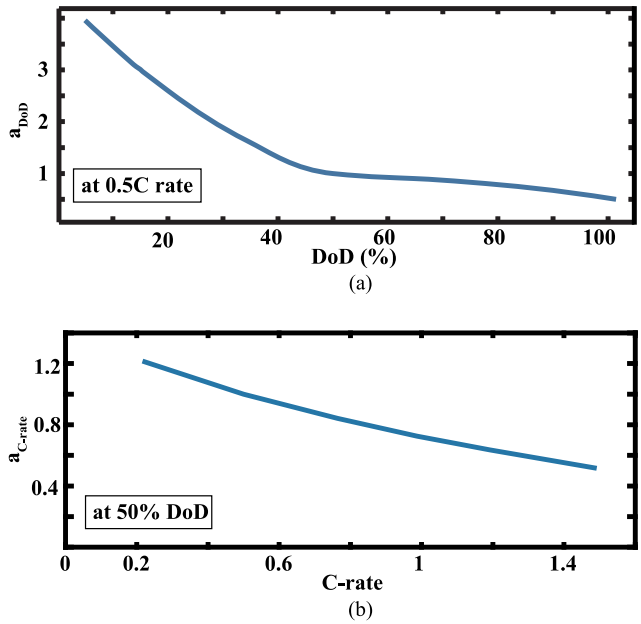


Fig. 4. Variation of (a) the parameter $a_{\mathrm{DoD}}$ versus DoD and (b) parameter $a_{C\text{-rate}}$ versus C-rate, considering the typical characteristic curves of the Li-ion BT of Fig. 3(a) and (b), respectively, for constant operating temperature 35 °C.

is required, the above methods can be used in the proposed algorithm.

### C. Lifespan Model of a BSS

The BSS may play a crucial role on the nZEB performance to alleviate the impacts of the intermittent nature of the RES and reinforce the effective implementation of the EMS operations for peak energy shaving of the load demand, feed-in minimization and effective scheduling of the appliances' operation. On the other hand, the initial cost and the protection of the BT lifespan which considerably affects the maintenance and replacement costs, are important parameters that should be considered.

It is well known that, the number of the total equivalent lifecycles of a Li-ion BT highly depends on the DoD, the nominal state-of-charge (SoC), the rate of the discharge depth, and the operating temperature [39], [40]. Typical characteristic curves of the energy capacity variation versus the total equivalent lifecycles, with respect to the DoD and C-rate, for constant operating temperature of 35 °C [41], are illustrated in Figs. 3(a) and (b), respectively.

It is usually considered that, a Li-ion BT has reached the end-of-life when its energy capacity has been degraded to 80% of its nominal value. Thus, in order to quantify the impacts of the DoD and C-rate with respect to the equivalent life-time cycles, the following parameters are defined, respectively, for constant temperature operating conditions

$$a_{\mathrm{DoD}} = \frac{LC^{\mathrm{DoD}}_{\mathrm{cap}=80\%}}{LC^{\mathrm{DoD}=50\%}_{\mathrm{cap}=80\%}} \tag{7}$$

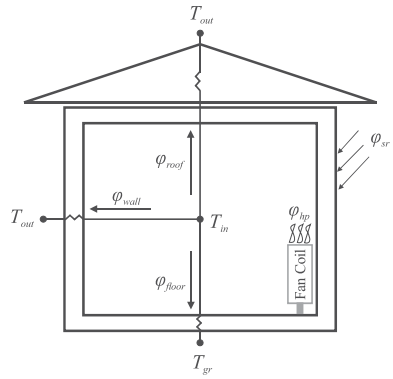


Fig. 5. Thermal model of an nZEB.

and

$$a_{C-\mathrm{rate}} = \frac{LC^{C-\mathrm{rate}}_{\mathrm{cap}=80\%}}{LC^{0.5C}_{\mathrm{cap}=80\%}} \tag{8}$$

where $LC^{\mathrm{DoD}}_{\mathrm{cap}=80\%}$ and $LC^{C-\mathrm{rate}}_{\mathrm{cap}=80\%}$ are the BT's life cycles that are realized with any given DoD and C-rate values, respectively, when the energy capacity has been reduced to 80%, and $LC^{\mathrm{DoD}=50\%}_{\mathrm{cap}=80\%}$ and $LC^{0.5C}_{\mathrm{cap}=80\%}$ are the BT's life cycles that are realized with DoD equal to 50% and operation with 0.5C, respectively, when the energy capacity has been reduced to 80%. Considering the above definitions, the variation of the $a_{\mathrm{DoD}}$ with respect to the DoD, for operation at 1C and 35°C, for the Li-ion BT data of Fig. 3(a), is illustrated in Fig. 4 (a). Also, the variation of the $a_{C-\mathrm{rate}}$ with respect to the C-rate, for operation at 50% DoD and 35 °C, for the Li-ion BT data of Fig. 3(b), is illustrated in Fig. 4(b).

The above capability factors for the BT's life cycles are defined with respect to 50% of DoD and operation with 0.5C, since they correspond to the mean BT operating conditions. Thus, the total lifetime capacity $Q_{bt}$ can be estimated by the following formula:

$$Q_{bt} = Q_{br}\, a_{C-\mathrm{rate}}\, a_{\mathrm{DoD}}\, LC_r \tag{9}$$

where $Q_{br}$ is the nominal capacity and $LC_r$ is the rated number of the lifetime cycles that corresponds to $a_{C-\mathrm{rate}} = a_{\mathrm{DoD}} = 1$. The total operating period of a Li-ion BT until it should be replaced ($T_{\mathrm{rep}}$) can be determined by considering that

$$Q_{bt} = \int_0^{T_{\mathrm{rep}}} (P_{\mathrm{ch}} + P_{\mathrm{dis}})dt \tag{10}$$

where $P_{\mathrm{ch}}$ and $P_{\mathrm{dis}}$ are the instantaneous BT's charge and discharge power, respectively.

### D. Thermal Model of a ZEB

Since the heating/cooling system has important role for both the nZEB performance and residents' comfort, the usage of the thermal model is needed to estimate the energy requirements. Several methodologies to evaluate the thermal requirements of a building have been proposed in the literature, such as [42], [43]. A physical model of a simple building envelop is considered in this article, where the thermal energy can be transferred through the walls, floor and roof. However, any other thermal model can be used as well, a simpler or a highly detailed model, depending on the type of the building and the potential requirements to model specific construction details, the computational complexity, the availability of the model's data and the desired accuracy in the results.

For every *i*-surface, the thermal flow is calculated by [44]

$$\varphi_i = \frac{T_{\mathrm{in}} - T_{\mathrm{out}}}{R^i_{\mathrm{cond}}} \tag{11}$$

where $T_{\mathrm{in}}$ and $T_{\mathrm{out}}$ are the indoor and outdoor air temperature, respectively, and $R^i_{\mathrm{cond}}$ is the thermal conduction resistance of every *i*-surface that is defined as

$$R^i_{\mathrm{cond}} = \frac{x_w}{k \cdot A} \tag{12}$$

where $A$ is the area of the surface, $k$ is the thermal conductivity, and $x_w$ is the thickness of the surface.

The solar radiation thermal flow is determined by

$$\varphi_{sr} = h_0\, A\, [T^{\mathrm{eq}}_{\mathrm{out}} - T_{\mathrm{surr}}] \tag{13}$$

where

$$T^{\mathrm{eq}}_{\mathrm{out}} = T_{\mathrm{out}} + \frac{a_s \varphi_{\mathrm{solar}}}{h_0} - \frac{\varepsilon\sigma[T^4_{\mathrm{out}} - T^4_{\mathrm{surr}}]}{h_0} \tag{14}$$

and $h_0$ is the combined convection and radiation heat transfer coefficient, $\alpha_s$ is the solar absorption coefficient, $\varphi_{\mathrm{solar}}$ is the solar radiation incident on the surface, $\varepsilon$ is the emissivity of the surface, $\sigma$ is the Stefan-Boltzmann constant, $T^{\mathrm{eq}}_{\mathrm{out}}$ is the equivalent outdoor air temperature due to the solar radiation effect in an exposed surface, and $T_{\mathrm{surr}}$ is the average temperature of the surrounding surface.

Considering the above, the thermal flow of the heat pump can be calculated by

$$\varphi_{\mathrm{hp}} = \frac{m_a c_p (T_{\mathrm{in}} - T_{\mathrm{out}})}{\Delta t} - \varphi_{sr} + \varphi_{\mathrm{walls}} + \varphi_{\mathrm{floor}} + \varphi_{\mathrm{roof}} \tag{15}$$

where $m_a$ and $c_p$ are the mass and the heat capacity of the air in the building, respectively, and $\Delta t$ is the time interval of each step of the calculation algorithm. Thus, the electric energy consumption of the heat pump to keep the indoor temperature to the desired setpoint is given by

$$P_{hp} = |\varphi_{hp}| \cdot \ CoP \tag{16}$$

where CoP is the coefficient-of-performance of the HP during heating and cooling operation.

### E. Modeling of the Impact of the EMS's Performance

The impact of the EMS's performance on the sizing of the nZEB 's equipment is considered through a virtual model that emulates the operation of the PAs and CAs, by examining several scenarios of energy management, so as, peak shaving of the load energy is attained through the proper time scheduling of the PAs and the effective control of the indoor temperature by the proper regulation of the CAs. Also, the exploitation of the EMS and BSS is taken into account through another virtual model that examines several operating conditions of the proper management of the electric energy generated by the RES, i.e., self-consumption within the nZEB, supply to the grid and temporary storage in the BSS.

The EMS control strategy of the [10] has been adopted in this article to calculate the energy consumption of the PAs and CAs, and consider the exploitation level of the RES and BSS, since it takes into account two important operating parameters, i.e., the residents' comfort and the tariff energy policy. The energy consumption of the UAs is obtained by historical data.

### F. Modeling of the Economic Aspect of the Problem

The economic aspect of the problem for converting a conventional building to nZEB can be considered through its two main features, i.e., the initial investment cost that refers to the purchase cost of the equipment and the availability cost which comprises the maintenance, utilization and replacement costs. The above have dual roles, directly through economic impacts for determining the correct sizing of nZEB's equipment and indirectly by influencing several installation parameters that are related with the proper configuration of the nZEB's microgrid. As an example, Figs. 6(a) and (b), illustrates typical purchase cost curves for RES and BSS, respectively [45]. Specifically, Fig. 6(a) shows the variation of the RES purchase cost with respect to the nominal power and Fig. 6(b) shows the variation of the BSS purchase cost versus both the nominal power and energy capacity.

Except for the initial investment cost, considerable impact on the correct sizing of the nZEB's equipment has the energy that is exchanged between the main grid and the nZEB, since it significantly influences the exploitation factor of the whole

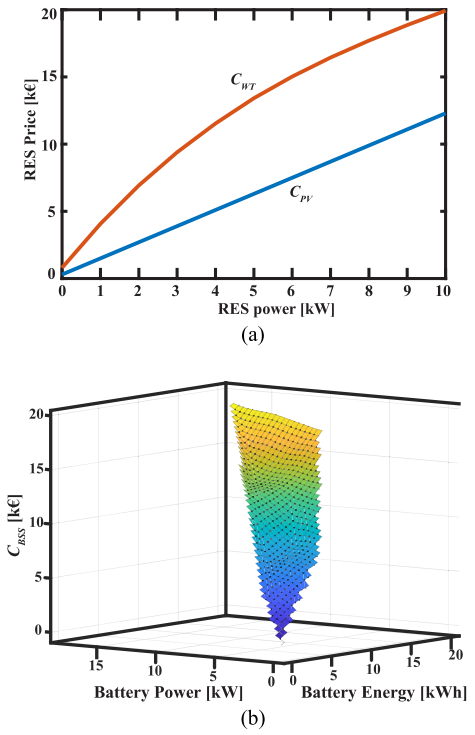


Fig. 6. Typical characteristic curves of the investment cost. (a) Purchase cost of the RES versus nominal power. (b) Purchase cost of the BSS versus nominal power and energy capacity.

nZEB's infrastructure. Specifically, it directly affects the depreciation period and it is indirectly tangled with the performance and consequently, the efficiency of the nZEB's microgrid. The above are taken into account at the optimization process of the nZEB's equipment through the parameters $C_{\text{sell}}$ and $C_{\text{buy}}$ that refer to the cost of the energy provided and absorbed by the grid, respectively. Note that the above energy cost parameters can be considered either as fix prices for the whole optimization horizon or, for increasing the accuracy of the calculation outcome, they can be considered as time-varying values, i.e., $C_{\text{sell}}(t)$ and $C_{\text{buy}}(t)$.

## IV. Cost Function Formulation

The role of the cost function is to embody the impacts of the most important parameters that affect the nZEB performance and therefore, they can be considered as the basis for the determination of the sizing of the required equipment. Thus, the cost function is defined through several economic and operating factors and also, some constraints are introduced to assist the optimization process and also to ensure that the enhanced algorithm is resulted to a feasible solution.

### A. Economic Impact

The cost is an important factor, since it considerably affects the decision of the householder to proceed on converting his house to nZEB and also, influences several other optimization variables. Thus, the economic impact can be included in the optimization process through the cost factor $F_{\text{cost}}$ that is defined as the ratio of the total investment cost with respect to the operating cost of the building. Thus, the $F_{\text{cost}}$ is defined by the following formula

$$F_{\text{cost}} = \frac{C_{\text{PV}} + C_{\text{WT}} + C_{\text{BSS}_{\text{Con}}} + a_{\text{rep}} C_{\text{BSS}_{\text{BT}}}}{C_{\text{oper}} H} \tag{17}$$

where $C_{\text{PV}}$ and $C_{\text{WT}}$ are the purchase costs of the PV and WT systems, respectively, $C_{\text{BSS}_{\text{Con}}}$ is the cost of all the BSS components except the BTs' cost, while $C_{\text{BSS}_{\text{BT}}}$ is the BTs' cost. The $C_{\text{oper}}$ is the annual cost of the energy consumed by the appliances, prior the building is converted to nZEB, and the $H$ is the optimization horizon in years. The parameter $a_{\text{rep}}$ is used to penalize the replacement of the BTs and hence, it increases accordingly the $C_{\text{BSS}_{\text{BT}}}$ cost. Thus, it is defined by

$$a_{\text{rep}} = H \backslash T_{\text{rep}} + \left[1 - \frac{1 - H \bmod T_{\text{rep}}}{a_{\text{rep}}^{\text{cost}}}\right] \quad , \quad a_{\text{rep}}^{\text{cost}} \geq 1 \tag{18}$$

where $T_{\text{rep}}$ is the replacement time calculated by (10) and $a_{\text{rep}}^{\text{cost}}$ is a parameter chosen by the designer and governs how the replacement cost of the BTs is considered in the optimization algorithm. The \ and mod symbols represent the integer division and the modulo function, respectively.

If it is selected $a_{\text{rep}}^{\text{cost}} \to \infty$, it means that the last replacement cost of the BTs is fully billed in the total cost of the system, regardless the BTs have been exhausted or not within the calculation period $H$, and thus, the (18) becomes

$$a_{\text{rep}} = H \backslash T_{\text{rep}} + 1. \tag{19}$$

On the other hand, if $a_{\text{rep}}^{\text{cost}} > 1$, a percentage of the last replacement of the BTs is considered in the full cost of the system. Specifically, the higher value the $a_{\text{rep}}^{\text{cost}}$, the lower percentage of the last BTs' replacement cost is considered.

### B. Depreciation Factor

For many households, the depreciation period is equally important, or sometimes more significant than the initial investment cost. Thus, the depreciation factor for the nZEB's equipment $F_{\text{dep}}$ is gauged on the basis of an optimization horizon of $H$ years and it is defined as

$$F_{\text{dep}} = \frac{T_{\text{dep}}}{H} = \frac{C_{\text{PV}} + C_{\text{WT}} + C_{\text{BSS}_{\text{Con}}} + a_{\text{rep}} C_{\text{BSS}_{\text{BT}}}}{\left(C_{\text{init}} + \int_y P_{\text{sell}}(t) C_{\text{sell}}(t) dt - \int_y P_{\text{cons}}(t) C_{\text{buy}}(t) dt\right) H} \tag{20}$$

where $P_{\text{cons}}(t)$is the electric power absorbed by the main grid and consumed within the nZEB's microgrid and $P_{\text{sell}}(t)$ is the electric power provided to the grid by the nZEB. The symbol $y$ in the integrals means that they are calculated on a year basis. Thus, the numerator of the $F_{\text{dep}}$ is the sum of the initial investment cost and the replacement cost of the BTs, while the denominator is the operating cost of the building, on the basis of $H$ years, considering the cost of the energy exchanged with the main grid (namely, selling energy minus buying energy by the grid).

### C. Exchange Energy With the Grid

Although the reduction of energy consumption and the increase of the energy generation by RES are very important toward the effort in the decarbonization of the energy systems, the injection to the grid of the excess energy generated by RES in an nZEB may be subjected to several restrictions imposed by the energy manager and the energy provider. Since this may affect the exploitation of the nZEB's equipment, a cost factor that considers the exchange energy between nZEB and main grid is applied in the optimization algorithm and is given by

$$F_{\text{grid}} = \frac{\int_H P_{\text{sell}}(t)dt}{\int_H P_{\text{load}}(t)dt} \tag{21}$$

where $P_{\text{sell}}$ is the power provided to the grid and $P_{\text{load}}$ is the power demanded by the nZEB's loads, both on per $H$ years basis.

### D. Peak Power Shaving

The ability of the nZEB's equipment for effective peak power shaving is an important feature, since it can reduce the operating cost of the building and increase the utilization of the energy generated by the RES. Thus, the peak power saving factor $F_{\text{peak}}$ is defined, on per $H$ years basis (namely for the 365 days $d$ of a year), as the average value of the ratio of the peak power consumption absorbed by the main grid $P_{\text{cons}}^{\text{peak}}$ to the peak power of the nZEB's loads $P_{\text{load}}^{\text{peak}}$, as given by the following formula

$$F_{\text{peak}} = \frac{\sum_{d=1}^{365H} \frac{P_{\text{cons}}^{\text{peak}}(d)}{P_{\text{load}}^{\text{peak}}(d)}}{365H}. \tag{22}$$

The aforementioned $F_{\text{peak}}$ factor acts complementary to the $F_{\text{grid}}$, since it is highly related to the exchange of electric energy between the nZEB and the main grid and thus, indirectly influences the cost and the depreciation factors, $F_{\text{cost}}$ and $F_{\text{dep}}$, respectively.

### E. Contribution of the RES

The RES size in respect to the nZEB's loads is a key index for the effectiveness and the exploitation of the selected equipment. It is highly related with all the above factors and its impact on the optimization process can be quantified through the RES factor $F_{\text{RES}}$. It is defined as the ratio of the energy generated by the RES to the energy demanded by the loads throughout the optimization horizon $H$ years

$$F_{\text{RES}} = \frac{\int_H P_{\text{RES}}(t)dt}{\int_H P_{\text{load}}(t)dt} \tag{23}$$

where

$$P_{\text{RES}} = P_{\text{WT}e} + P_{\text{PV}e}. \tag{24}$$

### F. Energy Autonomy by the Grid

The last factor that is involved in the optimization process for the sizing of the nZEB's equipment relates with the desired energy autonomy level of the building. Specifically, the energy autonomy factor $F_{\text{aut}}$ is defined as the ratio of the energy consumption of the nZEB absorbed by the main grid to the energy demand of the loads throughout the optimization horizon $H$ years

$$F_{\text{aut}} = \frac{\int_H P_{\text{cons}}(t)dt}{\int_H P_{\text{load}}(t)dt}. \tag{25}$$

### G. Cost Function

All the above factors constitute the following cost function that is minimized through the optimization process

$$CF = k_{\cos t}F_{\text{cost}} + k_{\text{dep}}F_{\text{dep}} + k_{\text{grid}}F_{\text{grid}} + k_{\text{peak}}F_{\text{peak}} + k_{\text{RES}}F_{\text{RES}} + k_{\text{aut}}F_{\text{aut}} \tag{26}$$

where $k_{\text{cost}}$, $k_{\text{dep}}$, $k_{\text{grid}}$, $k_{\text{peak}}$, $k_{\text{RES}}$, and $k_{\text{aut}}$ are the respective weighting factors that are selected by the designer of the nZEB according to his preferences and the technical characteristics of the nZEB, to weight the contribution of each factor to the optimization result. The sum of all the above weighted factors should be equal to one.

Note that, several of the input parameters in the sizing algorithm vary by the time, such as the cost of energy, BSS replacement cost, SoH of the battery, values of the thermal model, efficiency of the PV and WT, climate conditions, etc. Thus, if a more precise and detailed calculation of the correct sizing of the RES and BSS is required, the input parameters can be given as functions with respect to the time. In this case, the proposed algorithm can provide the correct sizing of the RES and BSS for a specific time horizon of $H$ years, by considering the dynamic variation of the input variable with the time.

### H. Constraints on the Cost Function

In order to accelerate the algorithm's solution process by reducing the iterations needed for converging to the solution, facilitate the calculations to provide a solution within acceptable operating conditions, and restrict the solutions space to feasible results, the following constraints have been imposed.

*1) Nominal Power of the RES:* The sum of the nominal power of the RES (PVs and WTs) should not be much greater than the average peak power of the nZEB's loads. Thus, the parameter $a_{\text{RES}}$ is introduced to give the designer the flexibility to properly adjust the above constraint in the optimization algorithm. Hence,

$$c_{\text{RES}}: \quad P_{\text{PV}} + P_{\text{WT}} \leq a_{\text{RES}} \frac{\sum_{d=1}^{365H} P_{\text{load}}^{\text{peak}}(d)}{365H}, \; a_{\text{RES}} > 0. \tag{27}$$

Note that the increase of the $a_{\text{RES}}$ parameter results to the increase of the constraint on the nominal power of the RES with respect to the average annual peak power of the nZEB's loads.

*2) Installation Space:* When deploying the RES in residential areas, the limited space availability should be considered [46]. The above is materialized through the following constraint:

$$c_{\text{space}}: \quad A_{\text{PV}}(P_{\text{PV}}) + A_{\text{WT}}(P_{\text{WT}}) \leq A_{\text{avail}} \tag{28}$$

where $A_{\text{PV}}()$ is a function of the required space per PV installed power $P_{\text{PV}}$, $A_{\text{WT}}()$ is a function of required space per WT installed power $P_{\text{WT}}$, and $A_{\text{avail}}$ is the available space for the whole RES installation.

In this article, it is assumed that all the PV modules have been installed at the same planar surface, either on a dedicated base, or directly onto the inclined roof, and thus we have

$$A_{\mathrm{PV}}(P_{\mathrm{PV}}) = \frac{P_{\mathrm{PV}}}{\eta_{\mathrm{PV},A}} \cos\theta \tag{29}$$

where $\eta_{\mathrm{PV},A}$ is the PV modules efficiency [in $\mathrm{W}_p/\mathrm{m}^2$] and $\theta$ is the inclination angle of the installation position. Since, Darrieus-type WT is considered in this article, we have

$$A_{\mathrm{WT}} = D_{\mathrm{WT}} * h_{\mathrm{WT}} \tag{30}$$

where $D_{\mathrm{WT}}$ is the rotor diameter and $h_{\mathrm{WT}}$ is the height of the blades. For safety and effective operation purposes, a ground area of a cycle of radius $L_s$ around the WT is considered, and thus

$$A_{\mathrm{WT}}(P_{\mathrm{WT}}) = \left( \frac{2P_{\mathrm{WT}}}{\rho C_{P_{\max}} u_h^3 h_{\mathrm{wt}}} + 2L_s \right)^2 \tag{31}$$

*3) Nominal Power of the BSS:* It is well known that the charging and discharging of BTs are usually realized by the commercially available technologies with 1C rate. Therefore, the solution space for the nominal power of the BT system $P_{\mathrm{BSS}}$ should be limited according to the nominal energy capacity $E_{\mathrm{BSS}}$

$$c_{P_{\mathrm{BSS}}}: \quad \begin{cases} P_{\mathrm{BSS}} \le \frac{E_{\mathrm{BSS}}}{3600}, & E_{\mathrm{BSS}} > 0 \\ P_{\mathrm{BSS}} = 0, & E_{\mathrm{BSS}} = 0. \end{cases} \tag{32}$$

*4) Nominal Energy Capacity of the BSS:* The BSS is used to temporary storing the energy generated by the RES and thus, to properly utilize it in order to effectively attain peak power shaving on the building loads' power demand. Therefore, the required energy capacity of a BT system $E_{\mathrm{BSS}}$ on a daily basis ($d$), should be confined by the maximum energy generated by the RES

$$c_{E_{\mathrm{BSS}}}: \quad E_{\mathrm{BSS}} \le a_{E_{\mathrm{BSS}}} \max \left[ \int_d (P_{\mathrm{WT}e} + P_{\mathrm{PV}e})\, dt \right]$$
$$a_{E_{\mathrm{BSS}}} > 0. \tag{33}$$

In the above constraint, the parameter $a_{E_{\mathrm{BSS}}}$ is selected by the nZEB's designer according to the importance that may be given to the BSS role as an interface between the RES and the main grid for temporarily energy storing.

*5) Limitation in the PAs Shifting:* Finally, as mentioned in Section III, the proposed enhanced algorithm of the sizing of the nZEB's equipment considers the performance of the EMS by adopting the control strategy of the PAs, CAs, RES and BSS of [10]. The above is realized through a virtual model of the operation of the aforementioned devices.

However, since the comfort of the residents should be considered, the shifting of the PAs is under specific constraints that are imposed by the residents' preferences. Specifically, the acceptable shifting margin of each PA is defined at the virtual model of the nZEB's microgrid by the residents, through the starting and ending time $T_a$ and $T_b$, respectively

$$c_{\mathrm{PA}}: \quad \{T_a, T_b\} \quad \text{for each } PA. \tag{34}$$

In order to be more explicit, an example of the PAs acceptable shifting with the EMS of [10], over a day in an nZEB, is illustrated in Fig. 7. The solid lines correspond to the time intervals of the PAs' operation with the EMS and the dashed lines depict the acceptable shifting limits imposed by the residents' preferences.

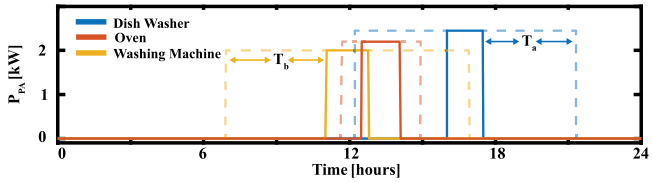


Fig. 7. Operation of the appliances of the nZEB for an arbitrarily selected day (the solid lines correspond to the time interval of the PAs' operation decided by the EMS of [10], while the dashed lines refer to the acceptable shifting limits imposed by the residents' preferences).

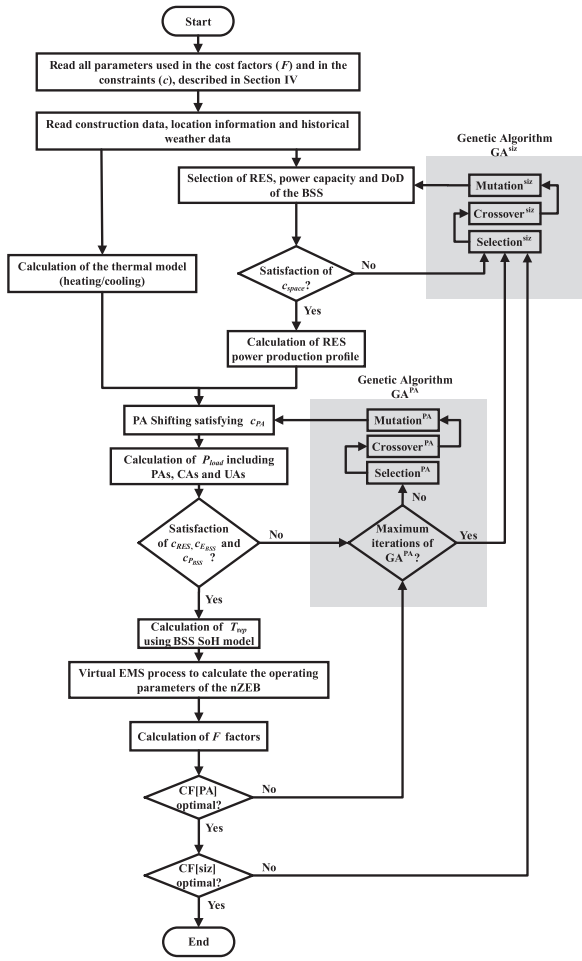


Fig. 8. Flowchart of the proposed sizing calculation algorithm of the RES and BSS in a nZEB.

## V. Proposed Sizing Algorithm

The proposed algorithm of the nZEB's sizing equipment is based on the GA technique and it is illustrated in Fig. 8. The solution is determined by utilizing two GAs that are interconnected in a nested form. In particular, the $GA^{siz}$ finds the size

of the RES and the BSS by minimizing the CF with respect to the cost factors and considering several predefined constraints. The GA$^{PA}$ improves the solution of the calculation process of the GA$^{siz}$ by considering the performance of the energy management of the nZEB's microgrid. In other words, the GA$^{PA}$ operates in an inner loop as a further investigation for assuring the optimal solution of the outer loop of GA$^{siz}$. Specifically, the GA$^{PA}$ investigates if each candidate solution of the GA$^{siz}$ can be improved through a virtual EMS by finding the optimal time shifting of the PAs, so as, both nZEB's loads demand and residents' comfort are satisfied. Thus, for every evolution step of the GA$^{siz}$, the GA$^{PA}$ is called, and when it finds the suitable time-table for the operation of the PAs, then the GA$^{siz}$ resumes its operation. The convergence and the termination of the inner GA$^{PA}$ is decided by the minimization of the cost function CF[PA] and specifically, the maximum number or iterations, the fitness limit and the fitness tolerance The same holds for the convergence of the outer genetic algorithm GA$^{siz}$, but for each best solution (as defined above) of the GA$^{PA}$. Therefore, the GA$^{siz}$ always converge to an optimal solution that is the correct sizing of the RES and BSS, and consequently, this is the termination of the whole calculation algorithm.

As can be seen in Fig. 8, the optimization algorithm initiates by reading the parameters which then are used for the modeling and solving of the optimization procedure. Also, the weather data and the detailed constructional characteristics are imported to the algorithm. Using the above data and considering the model of the heating and cooling system, the power consumption for the nZEB's heating and cooling are calculated.

The iteration procedure for the GA$^{siz}$ is initiated by arbitrarily selecting a set of $P_{\mathrm{WT}}$, $P_{\mathrm{PV}}$, $E_{\mathrm{BSS}}$, $P_{\mathrm{BSS}}$, and DoD. Then, it is checked if the constraint of the installation space $c_{\mathrm{space}}$ is satisfied with respect to the RES selection; otherwise, the $P_{\mathrm{WT}}$ and $P_{\mathrm{PV}}$ are properly adapted until the above criterion is satisfied. Thus, the GA$^{siz}$ investigates for the optimal selection of RES and BSS, considering the heating/cooling energy consumption through the thermal model and the proper performance of the EMS. The latter is accomplished by the GA$^{PA}$ for a certain number of iterations, through the virtual time shifting of the PAs and considering the energy consumption of the CAs and UAs. In this stage, the constraints $c_{\mathrm{RES}}$, $c_{P_{\mathrm{BSS}}}$, and $c_{E_{\mathrm{BSS}}}$ are considered, while the constraint $c_{\mathrm{PA}}$ is included in the virtual EMS. Note also that the proper selection of the BSS is examined with respect to the SoH model.

For each candidate solutions of the GA$^{PA}$ and GA$^{siz}$, the cost factors are calculated. If the CF with respect to the nZEB's loads resulted by the inner loop GA$^{PA}$ is optimal, it is then examined if the CF with respect to the whole process resulted by the outer loop GA$^{siz}$ is optimal too. If both criteria hold, the algorithm is terminated and provides the optimal sizing for the RES and BSS. Otherwise, the flow of the algorithm returns to the GA$^{PA}$ and GA$^{siz}$ loops, respectively, initiating a new iteration processes for seeking the optimal solution.

## VI. Validation of the Proposed Sizing Algorithm

To validate the effectiveness and functionality of the proposed methodology to determine the correct sizing of RES and BSS, a pilot nZEB at an urban area at Macedonia, Greece, has been considered. The energy consumption data for a period of two years has been obtained by measurements at the examined building. The weather data for a period of ten years has been obtained by [47]. The buying price of the electric energy was considered fixed at 0.25€/kWh and the selling price, also fixed, at 0.06€ /kWh. The EMS of [10] was used and the optimization horizon $H$ was set at 10 years.

TABLE I
Constraints for the Optimization Process

| Constraints | $a_{RES}$ | $A_{avail}$ | $a_{E_{BSS}}$ | $T_a$ | $T_b$ |
|---|---|---|---|---|---|
| Values | 1.5 | 4.3 | 1 | 0h | 24h |

The constraint $a_{\mathrm{RES}}$ was set 1.5, which means that up to 1.5 times of the average annual peak power consumption of the nZEB's loads can be provided by the RES. The nominal power values of the PV and WT are confined by the available roof space $A_{\mathrm{avail}}$, that for the examined nZEB was 100m$^2$. The value 1 has been selected for the constraint $a_{E_{\mathrm{BSS}}}$ in order to ensure relatively high energy capacity for the BSS and thus, high energy autonomy for the nZEB, by providing the capability to temporarily storing in the BTs the daily energy generated by the RES. Finally, the PAs are left free to operate at the exact time intervals that have been decided by the EMS for the examined day. Thus, the optimization algorithm operates with the full EMS process and without being imposed any additional time constraints to the appliances by the users. The above constraints that are considered in the optimization algorithm are given in Table I.

Two representative cases of the variation of the CF versus $P_{\mathrm{PV}}$ and $P_{\mathrm{WT}}$ with respect to the selection of the weighting factors and the usage of the BSS are examined in Figs. 9 and 10. Specifically, equal weighted factors ($k_{\mathrm{cost}} = k_{\mathrm{dep}} = k_{\mathrm{grid}} = k_{\mathrm{peak}} = k_{\mathrm{RES}} = k_{\mathrm{aut}} = 1/6$) are selected in Fig. 9, while a set of weighting factors that increases the building's autonomy level against the main grid ($k_{\mathrm{aut}} = 0.5$ and $k_{\mathrm{cost}} = k_{\mathrm{dep}} = k_{\mathrm{peak}} = k_{\mathrm{RES}} = k_{\mathrm{grid}} = 0.1$)is considered in Fig. 10. In both figures, the EMS of [10] is considered for the proper management of the PAs through the virtual shifting of their operating time. Also, Figs. 9(a) and 10(a) correspond to the case that no BSS is used ($E_{\mathrm{BSS}} = 0$), while Figs. 9(b) and 10(b) are referred to the case that $E_{\mathrm{BSS}} = 5$ kWh, $P_{\mathrm{BSS}} = 5$ kW and DoD $= 80\%$. The lowest CF of each case in the above figures is noted by a black dot and the resulting values for the CF, as well as, the nominal power of the PV and WT, are reported.

From the above figures, it can be observed that the CF is more sensitive to the increase of the $P_{\mathrm{PV}}$ and $P_{\mathrm{WT}}$ for the case of equal weighted factors at 1/6 (see Fig. 9), compared to the case of $k_{\mathrm{aut}} = 0.5$ and $k_{\mathrm{cost}} = k_{\mathrm{dep}} = k_{\mathrm{peak}} = k_{\mathrm{RES}} = k_{\mathrm{grid}} = 0.1$ (see Fig. 10). This is due to the uncertainty with respect the economic benefits of selling the excess energy to the grid considering the alternative choices of self-consumption by the nZEB and the temporary storage to the BSS for exploiting the variations of the energy price. The above are considered at the CF through the impacts of the $F_{\mathrm{cost}}$ and $F_{\mathrm{dep}}$ factors against the influence of the $F_{\mathrm{aut}}$. Moreover, comparing Figs. 9 with 10 it can be seen

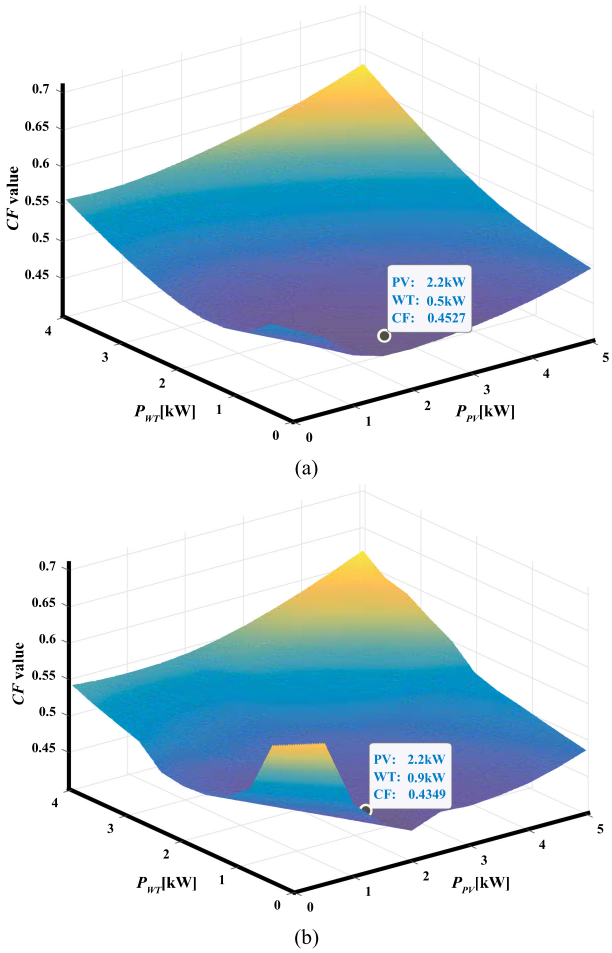


Fig. 9. Variation of the CF with respect to the $P_{\mathrm{PV}}$ and $P_{\mathrm{WT}}$, for equal weighted factors ($k_{\mathrm{cost}} = k_{\mathrm{dep}} = k_{\mathrm{grid}} = k_{\mathrm{peak}} = k_{\mathrm{RES}} = k_{\mathrm{aut}} = 1/6$), for the cases (a) $E_{\mathrm{BSS}} = 0$ and (b) $E_{\mathrm{BSS}} = 5$ kWh, $P_{\mathrm{BSS}} = 5$ kW, and DoD $= 80\%$.

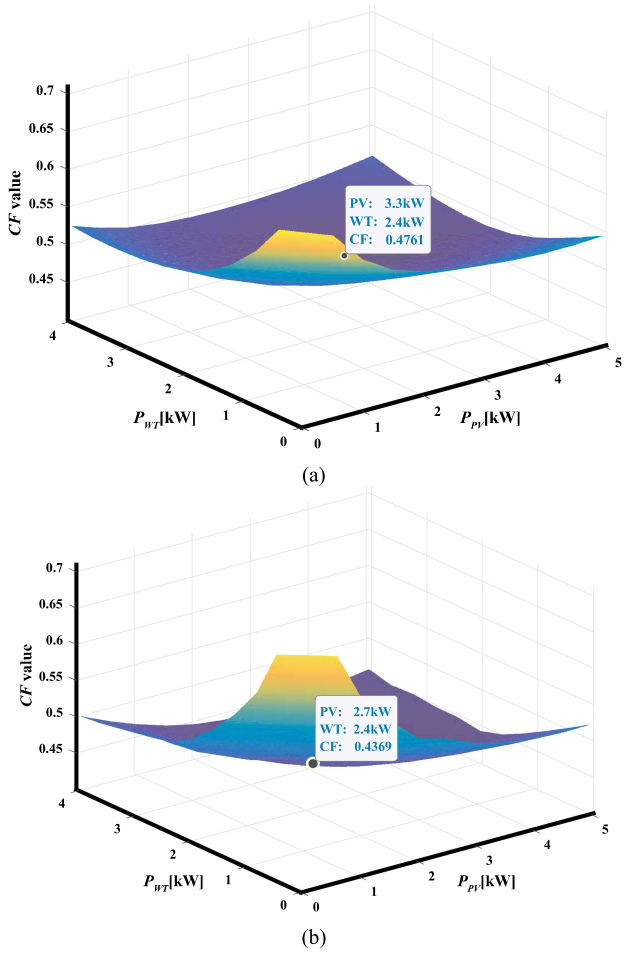


Fig. 10. Variation of the CF with respect to the $P_{PV}$ and $P_{WT}$, by selecting weighted factors that penalize the high interaction of the nZEB with the main grid ($k_{\mathrm{aut}} = 0.5$ and $k_{\mathrm{cost}} = k_{\mathrm{dep}} = k_{\mathrm{peak}} = k_{\mathrm{RES}} = k_{\mathrm{grid}} = 0.1$) , for the cases (a) $E_{\mathrm{BSS}} = 0$ and (b) $E_{\mathrm{BSS}} = 5$ kWh, $P_{\mathrm{BSS}} = 5$ kW, and DoD $= 80\%$.

that the use of the BSS lowers the CF for a wide selection of RES for both cases. This occurs because the BSS gives the ability to the EMS to manage the excess power production by the RES and thus, the interaction with the main grid can be reduced. Therefore, the variation with respect to the peak values and the cost of the energy consumption are smoothed and lowered, respectively. These result to the decrease of the $F_{\mathrm{grid}}$ factor, since the energy flow through the grid is reduced, while the $F_{\mathrm{aut}}$ is increased due to the increase of the nZEB energy autonomy level.

Fig. 11 illustrates calculation results from the optimization process for the case of equal weighted factors ($k_{\mathrm{cost}} = k_{\mathrm{dep}} = k_{\mathrm{grid}} = k_{\mathrm{peak}} = k_{\mathrm{RES}} = k_{\mathrm{aut}} = 1/6$) and the same scenarios for the BSS as in Fig. 9, but without considering the virtual time shifting of the PAs by the EMS. As can be seen, for both scenarios of BSS usage, higher nominal power for the RES is required when the EMS has been disregarded that results to worse CF values (see Fig. 11) compared to the case that the EMS is considered in the optimization process (see Fig. 9). The above validates the crucial role of considering the EMS in the optimization algorithm. Otherwise, overestimation in the sizing of the nZEB's equipment and consequently, worthless higher purchase cost would be resulted.

Note that, Figs. 9–11 illustrate the variation of the CF in a static form for the BSS selection. Thus, the resulted CF values are the local minimum, while the global minimum for each of the two examined cases of the weighted factors is provided by the optimization algorithm of Fig. 8 and the results are given in Table II. Specifically, Figs. 9–11 validate the effective performance of the optimization procedure for certain values of the BSS, as well as, the advantage of considering the EMS. Contrarily, the values at the Table II are obtained by the optimization algorithm of Fig. 8 which is an iterative procedure that seeks the optimal solution among a high number of combinations of $E_{\mathrm{BSS}}$, $P_{\mathrm{BSS}}$, and DoD and exploring the virtual load shifting of the PA, in order to give the lowest CF value for every candidate solution set.

The proposed method is compared with a conventional method that the RES and BSS sizing is determined by only considering the energy needs of the building and the results are given in Table II. The conventional method refers to the case that equal weighted factors are selected and thus, it can be evaluated

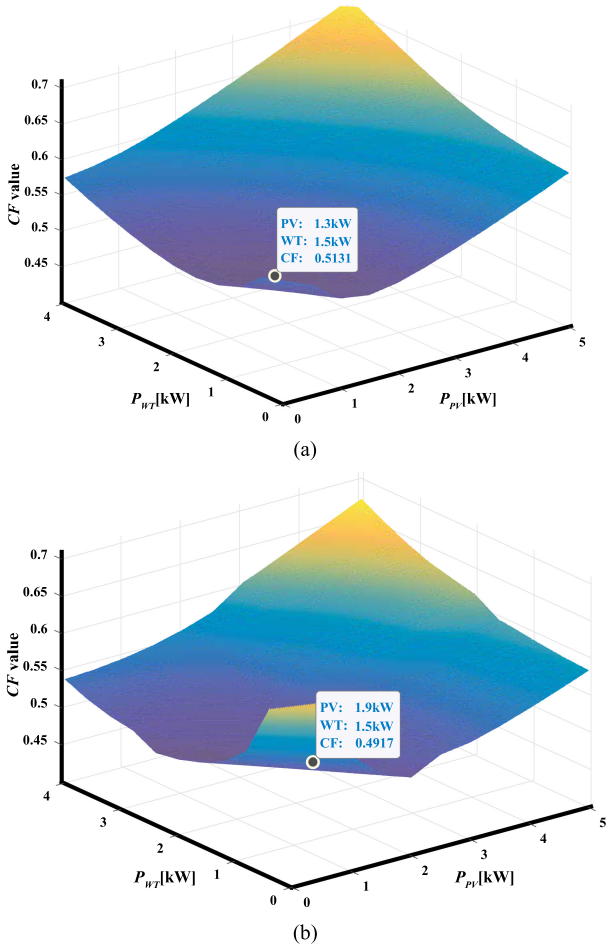


Fig. 11. Variation of the CF with respect to the $P_{\mathrm{PV}}$ and $P_{\mathrm{WT}}$, for equal weighted factors ($k_{\mathrm{cost}} = k_{\mathrm{dep}} = k_{\mathrm{grid}} = k_{\mathrm{peak}} = k_{\mathrm{RES}} = k_{\mathrm{aut}} = 1/6$)and without the virtual time shifting of the PAs, for the cases (a) $E_{\mathrm{BSS}} = 0$ and (b) $E_{\mathrm{BSS}}$ =5 kWh, $P_{\mathrm{BSS}} = 5$ kW, and DoD = 80%.

TABLE II
COMPARISON BETWEEN THE PROPOSED AND THE CONVENTIONAL ALGORITHMS

| Case / Variables | Proposed method | | Conventional method |
|---|---|---|---|
| | $k_{aut}$=$k_{cost}$=$k_{dep}$=$k_{RES}$ =$k_{grid}$=$k_{peak}$=1/6 | $k_{aut}$=0.5 & $k_{cost}$=$k_{dep}$ =$k_{RES}$=$k_{grid}$=$k_{peak}$=0.1 | $k_{aut}$=$k_{cost}$=$k_{dep}$=$k_{RES}$ =$k_{grid}$=$k_{peak}$=1/6 |
| $P_{PV}$ [kW] | 2.8 | 4.1 | 3.2 |
| $P_{WT}$ [kW] | 1.3 | 2.9 | 2 |
| $E_{BSS}$ [kWh] | 6.5 | 7.8 | 10.5 |
| $P_{BSS}$ [kW] | 2.8 | 4.1 | 6.1 |
| DoD [%] | 68 % | 77 % | 82 % |
| CF | 0.3812 | 0.414 | 0.473 |

the comparison between the respective case of the proposed method as well as the other case of the proposed method that the weighted factors refer to increased building's energy autonomy.

As can be seen, all the results of the equipment's sizing of the conventional method are higher compared with that of the proposed method for the case of equal weighted factors and thus, better CF value is attained with the proposed method. By

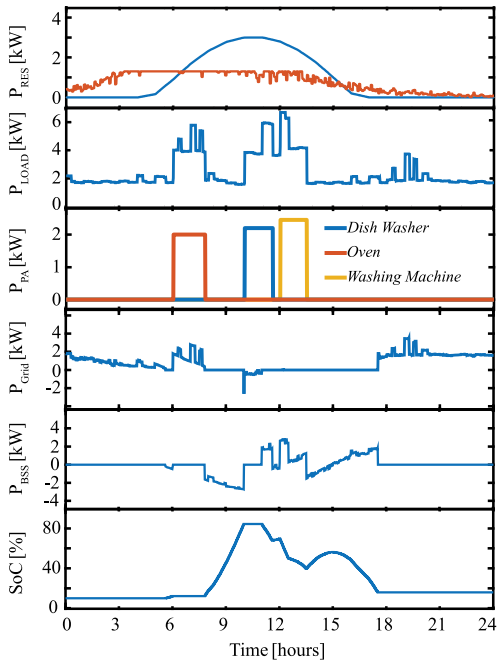


Fig. 12. Performance of the nZEB's microgrid for one day, for the case that the sizing of the RES and BSS is determined by the proposed method and for the case that equal weighted factors ($k_{\mathrm{cost}} = k_{\mathrm{dep}} = k_{\mathrm{grid}} = k_{\mathrm{peak}} = k_{\mathrm{RES}} = k_{\mathrm{aut}} = 1/6$) are considered, as in Fig. 9.

comparing the conventional with the proposed method for the case that the weighted factors correspond to the case of increased building's energy autonomy, the proposed algorithm results to higher sizing of the RES but lower values of the BSS and DoD. Moreover, since several operating and economic variables are disregarded in the conventional method, such as the EMS for the virtual time shifting of the PAs, the economic impact of the energy exchange with the grid, the contribution of the RES and the SoH of the BTs, it is resulted that improved CF value is attained with the proposed method in this case, too.

The performance of the examined nZEB for a typical autumn day are illustrated in Figs, 12–14, when the RES and BSS sizing is determined by the same cases that are compared in Table II. Specifically, Figs. 12 and 13 are referred to the proposed method for the cases that equal weighted factors and weighted factors that penalize the high interaction with the grid are selected, respectively, while Fig. 14 corresponds to the conventional method for the scenario that equal weighted factors is selected. The same wind speed and irradiance conditions are considered in all the examined cases.

By comparing Figs. 12 and 13, it can be seen that higher electric power is generated by the RES in the case of Fig. 13 compared to the case of Fig. 12, since the weighted factor of the energy autonomy kaut is higher. Although, for both cases, the PAs are properly scheduled by the EMS, higher energy is stored in the BSS at the case of Fig. 13 resulting to have 100% of SoC for a long-time interval during the day. Although the above results are only referred to one day and considering that the purchase cost of the equipment of Fig. 13 is higher due to their higher sizing, it is justified the worse CF value for the case of Fig. 13

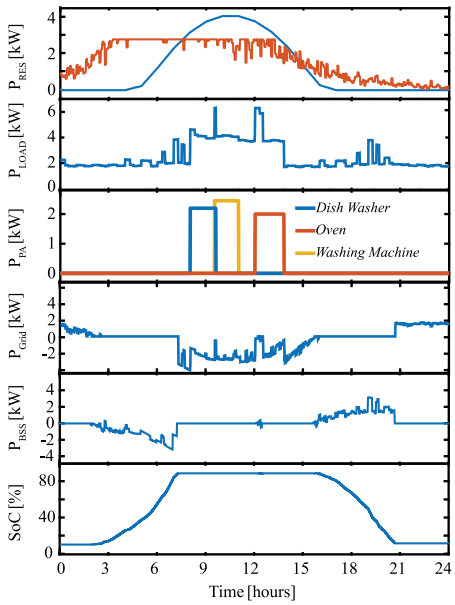


Fig. 13. Performance of the nZEB's microgrid for one day, for the case that the sizing of the RES and BSS is determined by the proposed method and for the case that the selection of the weighted factors increase the energy autonomy of the nZEB ($k_{\text{aut}} = 0.5$ and $k_{\text{cost}} = k_{\text{dep}} = k_{\text{peak}} = k_{\text{RES}} = k_{\text{grid}} = 0.1$), as in Fig. 10.

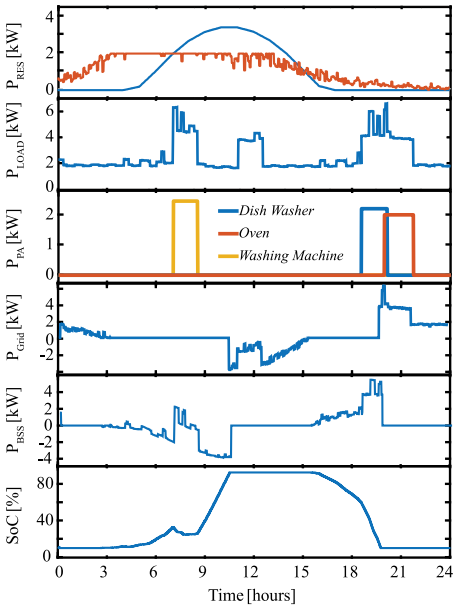


Fig. 14. Performance of the nZEB's microgrid for one day, for the case that the sizing of the RES and BSS is determined by a conventional method where only on the energy needs of the building are considered and corresponds to the scenario of equal weighted factors ($k_{\text{cost}} = k_{\text{dep}} = k_{\text{grid}} = k_{\text{peak}} = k_{\text{RES}} = k_{\text{aut}} = 1/6$).

compared to the case of Fig. 12 (see Table II). For the case of the conventional sizing method, it can be observed that higher electric energy is generated by the RES in Fig. 14 compared to the case of Fig. 12, but lower than the case of Fig. 13, since the sizing of the RES for the case of Fig. 14 is in the middle between the cases of Figs. 12 and 13 (see Table II). However, although the case of Fig. 14 of the conventional method has higher sizing of the BSS and DoD compared to the case of Fig. 13 of the proposed method, the lack of considering several operating and economic variables results to worse performance with respect to the BSS utilization for the case of Fig. 14 compared to that of Fig. 13(high exchange of energy with the grid).

## VII. Conclusion

In this article, a methodology for the correct sizing of the PV, WT, and BSS for the conversion of an existing building to nZEB has been presented. The proposed method considers both the technical and financial point of views of the problem to ensure the effective and efficient sizing of the needed nZEB's equipment. This is attained by taking into account several information for the weather, location, energy consumption, energy price as well as the EMS performance through impact factors and the optimal solution is provided by minimizing a cost function through the GA technique. Thus, the key benefit of the proposed method is the consideration of the most important parameters that may affect the sizing of the nZEB's equipment and therefore, and optimal solution for the problem is ensured. Selective calculation results that are referred to a real nZEB are presented, in order to validate the effectiveness and feasibility of the proposed method.

## References

[1] D. Kolokotsa, D. Rovas, E. Kosmatopoulos, and K. Kalaitzakis, "A roadmap towards intelligent net zero- and positive-energy buildings," *Sol. Energy,* vol. 85, no. 12, pp. 3067–3084, Dec. 2011.

[2] EU Directive 2018/2002 of 11 amending directive 2018/27/EU on energy efficiency, Dec. 2018, [Online]. Available: https://eur-lex.europa.eu/legal-content/EN/TXT/PDF/?uri=CELEX:32018L2002&from=EN

[3] EU Directive 2018/844 of 30 May 2018, "amending directive 2010/31/EU on energy performance of buildings," 2018, [Online]. Available: https://eur-lex.europa.eu/legal-content/EN/TXT/PDF/?uri=CELEX:32018L0844&from=EN

[4] Synthesis report on the national plans for nearly zero energy buildings (NZEBs), "European commission," 2016. [Online]. Available: https://publications.jrc.ec.europa.eu/repository/bitstream/JRC97408/reqno_jrc97408_online%20nzeb%20report(1).pdf

[5] F. Spertino, A. Ciocia, P. Di Leo, S. Fichera, G. Malgaroli, and A. Ratclif, "Toward the complete self-sufficiency of an nZEBs microgrid by photovoltaic generators and heat pumps: Methods and applications," *IEEE Trans. Ind. Appl.*, vol. 55, no. 6, pp. 7028–7040, Nov./Dec. 2019.

[6] J. Shi, W. Huang, N. Tai, P. Qiu, and Y. Lu, "Energy management strategy for microgrids including heat pump air-conditioning and hybrid energy storage systems," *J. Eng.*, no. 13, pp. 2412–2416, 2017.

[7] A. Ghalebani and T. K. Das, "Design of financial incentive programs to promote net zero energy buildings," *IEEE Trans. Power Syst.*, vol. 32, no. 1, pp. 75–84, Jan. 2017.

[8] R. Francisco, C. Roncero-Clemente, R. Lopes, and J. F. Martins, "Intelligent energy storage management system for smart grid integration," in *Proc. 44th Annu. Conf. IEEE Ind. Electron. Soc.*, pp. 6083–6087, 2018.

[9] M. A. Hannan *et al.*, "A review of internet of energy based building energy management systems: Issues and recommendations," *IEEE Access*, vol. 6, pp. 38997–39014, 2018.

[10] E. Tsioumas, N. Jabbour, M. Koseoglou, and C. Mademlis, "A novel control strategy for improving the performance of a nearly zero energy building," *IEEE Trans. Power Electron.*, vol. 35, no. 2, pp. 1513–1524, Feb. 2020.

[11] A. Merabet, K. Tawfique Ahmed, H. Ibrahim, R. Beguenane, and A. M. Y. M. Ghias, "Energy management and control system for laboratory scale microgrid based wind-pv-battery," *IEEE Trans. Sustain. Energy*, vol. 8, no. 1, pp. 145–154, Jan. 2017.

[12] U. Akram, M. Khalid, and S. Shafiq, "An innovative hybrid wind-solar and battery-supercapacitor microgrid system—Development and optimization," *IEEE Access*, vol. 5, pp. 25897–25912, 2017.
[13] K. Basaran, N. S. Cetin, and S. Borekci, "Energy management for on-grid and off-grid wind/PV and battery hybrid systems," *IET Renew. Power Gener.*, vol. 11, no. 5, pp. 642–649, Apr. 2017.
[14] F. Asdrubali, L. Evangelisti, C. Guattari, and G. Grazieschi, "Evaluation of the energy and environmental payback time for a NZEB building," in *Proc. IEEE Int. Conf. Environ. Elect. Eng., IEEE Ind. Commercial Power Syst. Eur.*, 2018, pp. 1–6.
[15] M. A. DERICHE, A. Hafaifab, and K. Mohammedia, "EPBT and CO2 emission from solar PV monocrystaline silicon," in *Proc. Int. Conf. Appl. Smart Syst. Conf.*, 2018, pp. 1–3.
[16] W. Kellogg, M. Nehrir, G. Venkataramanan, and V. Gerez, "Generation unit sizing and cost analysis for stand-alone wind, photovoltaic, and hybrid wind/PV systems," *IEEE Trans. Energy Conv.*, vol. 13, no. 1, pp. 70–75, Mar. 1998.
[17] L. Wang and C. Singh, "PSO-based multi-criteria optimum design of a gridconnected hybrid power system with multiple renewable sources of energy," in *Proc. IEEE Swarm Intell. Symp.*, 2007, pp. 250–257.
[18] A. S. O. Ogunjuyigbe, T. R. Ayodele, and O. A. Akinola, "Optimal allocation and sizing of PV/wind/split-diesel/battery hybrid energy system for minimizing life cycle cost, emission and dump energy of remote residential building," *Appl. Energy*, vol. 171, pp. 153–171, Jun. 2016.
[19] D. Thomas, O. Deblecker, and C. S. Ioakimidis, "Optimal design and techno-economic analysis of an autonomous small isolated microgrid aiming at high RES penetr ation," *Energy*, vol. 116, pp. 364–379, 2016.
[20] S. Mashayekh *et al.*, "Security-Constrained design of isolated multi-energy microgrids," *IEEE Trans. Power Syst.*, vol. 33, no. 3, pp. 2452–2462, May 2018.
[21] P. Yang and A. Nehorai, "Joint optimization of hybrid energy storage and generation capacity with renewable energy," *IEEE Trans. Smart Grid*, vol. 5, no. 4, pp. 1566–1574, Jul. 2014.
[22] C. S. Lai and M. D. McCulloch, "Sizing of stand-alone solar PV and storage system with anaerobic digestion biogas power plants," *IEEE Trans. Ind. Electron.*, vol. 64, no. 3, pp. 2112–2121, Mar. 2017.
[23] R. Atia and N. Yamada, "Sizing and analysis of renewable energy and battery system in residential microgrids," *IEEE Trans. Smart Grid*, vol. 7, no. 3, pp. 1204–1213, Mar. 2016.
[24] S. Mashayekh, M. Stadler, G. Cardoso, and M. Heleno, "A mixed integer linear programming approach for optimal DER portfolio, sizing, and placement in multienergy microgrids," *Appl. Energy*, vol. 187, pp. 154–168, 2017.
[25] I. Alsaidan, A. Khodaei, and W. Gao, "A comprehensive battery energy storage optimal sizing model for microgrid applications," *IEEE Trans. Power Syst.*, vol. 33, no. 4, pp. 3968–3980, Jul. 2018.
[26] R. Rajbongshi, D. Borgohain, and S. Mahapatra, "Optimization of PV-biomass-diesel and grid base hybrid energy systems for rural electrification by using HOMER," *Energy*, vol. 126, pp. 461–474, May 2017.
[27] L. Xu, X. Ruan, C. Mao, B. Zhang, and Y. Luo, "An improved optimal sizing method for wind-solar-battery hybrid power system," *IEEE Trans. Sustain. Energy*, vol. 4, no. 3, pp. 774–785, Jul. 2013.
[28] C. Marnay, G. Venkataramanan, M. Stadler, A. S. Siddiqui, R. Firestone, and B. Chandran, "Optimal technology selection and operation of commercial-building microgrids," *IEEE Trans. Power Syst.*, vol. 23, no. 3, pp. 975–982, Aug. 2008.
[29] K. Panagiotou, C. Klumpner, and M. Sumner, "Sizing guidelines for grid-connected decentralised energy storage systems: Single house application," *J. Eng.*, vol. 2019, no. 17, pp. 3802–3806, Jun. 2019.
[30] L. Zhou, Y. Zhang, X. Lin, C. Li, Z. Cai, and P. Yang, "Optimal sizing of PV and BESS for a smart household considering different price mechanisms," *IEEE Access*, vol. 6, pp. 41050–41059, 2018.
[31] R. Singh and R. C. Bansal, "Review of HRESs based on storage options, system architecture and optimisation criteria and methodologies," *IET Renew. Power Gener.*, vol. 12, no. 7, pp. 747–760, Jul. 2018.
[32] E. Hau, *Wind Turbines Fundamentals, Technologies, Application, Economics*, Munich, Germany: Springer, 2012.
[33] G. M. Masters, *Renewable and Efficient Electric Power Systems*, Hoboken, NJ, USA: Wiley, 2004.
[34] R. Belfkira, L. Zhang, and G. Barakat, "Optimal sizing study of hybrid wind/PV/diesel power generation unit," *Sol. Energy,* vol. 85, pp. 100–110, 2011.
[35] D. Wu, H. Zeng, C. Lu, and B. Boulet, "Two-Stage energy management for office buildings with workplace EV charging and renewable energy," *IEEE Trans. Transport. Electrif.,* vol. 3, no. 1, pp. 225–237, 2017.
[36] P. Trinuruk, C. Sorapipatana, and D. Chenvidhya, "Estimating operating cell temperature of BIPV modules in Thailand," *Renew. Energy*, vol. 34, pp. 2515–22523, 2009.
[37] C. S. Ioakimidis, L. J. Oliveira, and K. N. Genikomsakis, "Wind power forecasting in a residential location as part of the energy box management decision tool," *IEEE Trans. Ind. Inform.*, vol. 10, no. 4, pp. 2103–2111, Nov. 2014.
[38] C. S. Ioakimidis, S. Lopez, K. N. Genikomsakis, P. Rycerski, and D. Simic, "Solar production forecasting based on irradiance forecasting using artificial neural networks," in *Proc. 39th Annu. Conf. IEEE Ind. Electron. Soc.*, pp. 8121–8126, Nov. 2013.
[39] Y. Gao, J. Jiang, C. Zhang, W. Zhang, Z. Ma, and Y. Jiang, "Lithium-ion battery aging mechanisms and life model under different charging stresses," *J. Power Sources*, vol. 356, pp. 103–114, Jul. 2017.
[40] E. Hossain, D. Murtaugh, J. Mody, H. M. R. Faruque, M. S. Haque Sunny, and N. Mohammad, "A comprehensive review on second-life batteries: Current state, manufacturing considerations, applications, impacts, barriers & potential solutions, business strategies, and policies," *IEEE Access*, vol. 7, pp. 73215–73252, 2019.
[41] M. Eck er *et al.*, "Calendar and cycle life study of li (nimnco) o 2-based 18650 lithium-ion batteries," *J. Power Sources*, vol. 248, pp. 839–851, Feb. 2014.
[42] A. Bagheri, V. Feldheim, and C. S. Ioakimidis, "On the evolution and the application of the thermal network method for energy assessment in buildings," *Energies*, vol. 11, no. 4, pp. 1–20, Apr. 2018.
[43] R. a. A.-C. E. *American Society of Heating*, Atlanta, GA, USA: ASHRAE Handbook-Fundamentals, 2001.
[44] P. Scott, S. Thiebaux, M. V. D. Briel, and P. V. Hentenryck, "Residential demand response under uncertainty," in *Proc. Int. Conf. Princ. Pract. Constraint Prog.*, 2013, pp. 645–660.
[45] Renewable energy components, retail prices, 2020. [Online], Available: http://www.windandsun.co.uk/products.aspx#.X0EL-cgzaUk
[46] N. M. Kumar, P. Das, and P. R. Krishna, "Estimation of grid feed in electricity from roof integrated Si-amorph PV system based on orientation, tilt and available roof surface area," in *Proc. Int. Conf. Intell. Comput., Instrum. Control Technol.*, 2017, pp. 588–596.
[47] K. Lagouvardos *et al.*, "The automatic weather stations NOANN network of the national observatory of athens: Operation and database," *Geosci. Data J.*, vol. 4, no. 1, pp. 4–16, 2017.

**Evangelos Tsioumas** (Student Member, IEEE) was born in Kompotades Fthiotidas, Greece, on June 13, 1988. He received the Diploma degree in 2013 from the School of Electrical and Computer Engineering, Aristotle University of Thessaloniki, Thessaloniki, Greece, where he is currently working toward the Ph.D. degree in energy management optimization in microgrids.

His research interests include energy management in power systems, control optimization in microgrids, large-scale electric energy storage systems, and embedded systems design.

**Nikolaos Jabbour** was born in Thessaloniki, Greece, on December 4, 1988. He received the Dipl. Eng. and Ph.D. degrees in electrical and computer engineering from the Aristotle University of Thessaloniki, Thessaloniki, Greece, in 2012 and 2018, respectively.

Since 2018, he has been a Postdoctoral Researcher with the Electrical Machines Laboratory, School of Electrical and Computer Engineering, Aristotle University of Thessaloniki. His research interests include control optimization, electrical machines and drives, power electronics, embedded systems, renewable energy systems, smart grids and energy management in nearly zero energy buildings.

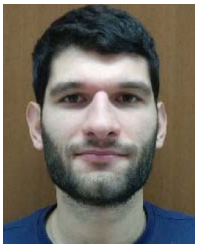

**Markos Koseoglou** (Student Member, IEEE) was born in Thessaloniki, Greece, on July 11, 1992. He received the Diploma degree in 2018 from the School of Electrical and Computer Engineering, Aristotle University of Thessaloniki, Thessaloniki, Greece, where he is currently working toward the Ph.D. degree in the area of battery management system optimization.

His research interests include energy management in power systems, battery management systems, and embedded systems design.

**Dimitrios Papagiannis** was born in Kranea Elassonas, Greece, on December 24, 1990. He received the Diploma degree in 2015 from the School of Electrical and Computer Engineering, Aristotle University of Thessaloniki, Greece, where he is currently working toward the Ph.D. degree in the area of optimization of vehicles' active suspension systems.

His research interests include performance improvement of active suspension systems in vehicles, vehicle dynamics, electric motor drives, power electronics and embedded systems design.

**Christos Mademlis** (Senior Member, IEEE) was born in Arnea Chalkidikis, Greece, on February 7, 1964. He received the Diploma degree in electrical engineering (first class hons.) and the Ph.D. degree in electrical machines from the Aristotle University of Thessaloniki, Thessaloniki, Greece, in 1987 and 1997, respectively.

Since 1990, he has been with the Electrical Machines Laboratory, Faculty of Electrical and Computer Engineering, Aristotle University of Thessaloniki, as a Research Associate (1990–2001), a Lecturer (2001–2006), an Assistant Professor (2007–2014), an Associate Professor (2014–2019), and is currently a Professor (since 2019). In 2013–2016, he has been the Head of the Department of Electrical Energy and since 2010, he has been the Director of the Electrical Machine Laboratory, Faculty of Engineering of the Aristotle University of Thessaloniki. He is author and co-author of more than 75 peer-reviewed technical papers. In 2013, he was the Founder, and for the Faculty Advisor from 2013 to 2017 with the Student Formula SAE racing team of the Aristotle University of Thessaloniki. In 2017, he was a Visiting Professor with the APED, Department of Electrical and Computer Engineering, University of Connecticut. His research interests include electrical machines and drives, especially in design and control optimization, renewable energy sources, electric vehicles, energy saving systems and energy management in nearly zero energy buildings